

Article (refereed)

Cox, Peter M.; Harris, Phil P.; Huntingford, Chris; Betts, Richard A.; Collins, Matthew; Jones, Chris D.; Jupp, Tim E.; Marengo, José A.; Nobre, Carlos A.. 2008 Increasing risk of Amazonian drought due to decreasing aerosol pollution. *Nature*, 453. 212-215. doi:10.1038/nature06960

Copyright 2008 Nature Publishing Group

This version available at <http://nora.nerc.ac.uk/2985/>

NERC has developed NORA to enable users to access research outputs wholly or partially funded by NERC. Copyright and other rights for material on this site are retained by the authors and/or other rights owners. Users should read the terms and conditions of use of this material at <http://nora.nerc.ac.uk/policies.html#access>

This document is the author's final manuscript version of the journal article, incorporating any revisions agreed during the peer review process. Some differences between this and the publisher's version remain. You are advised to consult the publisher's version if you wish to cite from this article.

<http://www.nature.com/nature/index.html>

Contact CEH NORA team at
nora@ceh.ac.uk

Increasing risk of Amazonian drought due to decreasing aerosol pollution

Peter M. Cox^{1,2}, Phil P. Harris³, Chris Huntingford³, Richard A. Betts², Matthew Collins², Chris D. Jones², Tim E. Jupp¹, José A. Marengo⁴, Carlos A. Nobre⁴

¹ *School of Engineering, Computer Science and Mathematics, University of Exeter, EX4 4QF, UK*

² *Hadley Centre, Met Office, Exeter, EX1 3PB, UK*

³ *Centre for Ecology and Hydrology, Wallingford, Oxon OX10 8BB, UK*

⁴ *Brazilian Centre for Weather Forecasting and Climate Studies, CPTEC/INPE, Sao Paulo, Brazil*

The Amazonian rainforest plays a crucial role in the climate system, helping to drive atmospheric circulations in the tropics by absorbing energy and recycling about half of the rainfall that falls upon it. The region is also estimated to contain about 10% of the carbon stored in land ecosystems, and to account for 10% of global net primary productivity¹. The resilience of the forest to the combined pressures of deforestation and global warming is therefore of great concern², especially since some General Circulation Models (GCMs) predict a severe drying of Amazonia in the 21st century^{3,4,5}. These climate projections are considered in the light of the 2005 drought in Western Amazonia, which was associated with unusually warm North Atlantic Sea-Surface Temperatures (SSTs)⁶. We show that reduction of dry season (July-October) rainfall in Western Amazonia is well-correlated with an index of north-south SST gradient across the equatorial Atlantic (“ANSG”). Our climate model is unusual amongst current GCMs in being able to reproduce this relationship and also the observed 20th Century multi-decadal variability⁷ in the ANSG when the effects of aerosols are included⁸. Simulations with the same model for the 21st Century^{3,8} show a strong tendency for the SST conditions associated with the 2005 drought to become much more common due to continuing reductions in reflective aerosol pollution in the northern hemisphere⁹.

In 2005 large areas of the Amazon river basin experienced one of the most intense drought episodes of the last 100 years⁶. The drought most directly affected Western Amazonia, and especially the catchments of the Solimões and the Madeiras Rivers. Navigation along these major tributaries had to be suspended because the water levels were so low. Unlike the El Niño related droughts in 1926, 1983 and 1997, central and eastern Amazonia were not directly affected, although river levels on the Rio Negro in central Amazonia did reach unusually low levels in October 2005 due to reduced inflow from the tributaries to the west.

Rainfall in Amazonia is sensitive to seasonal, interannual and decadal variations in SSTs^{7,10,11}. The warming of the tropical East Pacific during El Niño events suppresses wet-season rainfall through modification of the (East-West) Walker Circulation and via the Northern hemisphere extra-tropics¹². El Niño-like climate change¹³ has similarly been shown to influence annual mean rainfall over South America in GCM climate change projections^{4,5}.

However, variations in Amazonian precipitation are also known to be linked to SSTs in the tropical Atlantic¹¹. A warming of the tropical north Atlantic relative to the south leads to a north-westward shift in the Intertropical Convergence Zone (ITCZ) and compensating atmospheric descent over Amazonia¹⁰. For north-east Brazil the relationship between the north-south Atlantic SST gradient and rainfall is sufficiently strong to form the basis for a seasonal forecasting system¹⁴. Here we show that Atlantic SSTs exert a large influence on “dry-season” (July-October) rainfall in Western Amazonia by delaying onset of the South American Monsoon^{15,16}.

July to October 2005 was associated with a persistent warm-anomaly in the north Atlantic¹⁷ centred on 10-15°N, and a weaker cold anomaly in the south Atlantic at around 15°S (Figure 1). The absence of a warming in the tropical east Pacific implies that ENSO was in a near neutral state and therefore did not contribute to the 2005 drought. The black box over land in Figure 1 denotes the Western Amazonian area chosen for the purposes of this study (75°W-60°W, 12°S-

0°S). The black boxes over the ocean show the north (15°N-35°N, 75°W-30°W) and south (25°S-5°S, 40°W-5°E) regions used to calculate an index of the north-south SST gradient across the Atlantic (“Atlantic N-S Gradient (ANS_G)”). These areas were chosen for comparability with the GCM climate projections to be presented below, but are also near optimal based on a statistical analysis using observations alone¹⁸.

We analyse results from the HadCM3LC coupled climate-carbon cycle model⁴, which is based upon the Met Office Hadley Centre’s 3rd generation ocean-atmosphere general circulation model¹⁹. This is one of only three current global climate models which fits within the observational limits on the July-October West Amazonian rainfall and ANS_G (see Supplementary Information). The HadCM3 model has also performed well in GCM intercomparison exercises and was recently selected as one of two GCMs which simulate the Amazonian climate with reasonable accuracy⁵. HadCM3LC in addition includes dynamic vegetation and an interactive carbon cycle, so that atmospheric CO₂ concentrations can be updated based on anthropogenic emissions, taking account of the effects of climate change on ocean and land CO₂-uptake. We consider two separate simulations with HadCM3LC for the period from 1860 to 2100^{4,8}. In both cases the model is driven with CO₂ emissions consistent with the IS92a scenario, which is approximately in the centre of the spread of future emissions represented by the more recent SRES scenarios²⁰. Both model experiments also include prescribed time-varying concentrations of trace greenhouse gases (CH₄, N₂O) based on IS92a. The second run additionally includes changes in tropospheric and stratospheric ozone, solar variability, and most notably forcing from sulphate and volcanic aerosols. This model experiment was able to reproduce the observed warming and CO₂ increase over the 20th century to good accuracy, especially when a revised estimate of the net CO₂ flux from land-use change was used (run “ALL70” from ref. 8).

We compared the results from these simulations with observations of the ANS_G Index¹⁷ and rainfall in Western Amazonia²¹ for the 20th century, using 20 year running means in each case

(Figure 2). The 2005 ANSG Index value of 4.92 K was exceeded regularly during the 1930s, 40s and 50s, but has not reached such a high-value since 1960. There is significant variability in the 20-year mean ANSG Index (*i.e.* much larger than the standard-deviation of the annual mean values) with values declining from around 1960 to the mid-1980s, before increasing to higher-values in the last two decades. This variation is mirrored by the decadal-mean West Amazonian rainfall measurements, which declined from the 1920s to 1960, then increased until the mid-1980s before declining again to the values experienced today.

The two HadCM3LC simulations capture the observed inverse relationship between the ANSG Index and West Amazonian July-August-September-October (“JASO”) precipitation. However, the simulation with greenhouse gases only (red line in Figure 2) fails to reproduce the observed decadal variability in the ANSG Index (correlation coefficient between the 20 year running means of observed and modelled ANSG is -0.75), instead predicting a near-monotonic increase in the ANSG Index and a corresponding near-monotonic decrease in West Amazonian rainfall from the mid-20th century onwards. However, the HadCM3LC run with aerosols (green line in Figure 2) produces a good fit to the decadal variation in the ANSG Index (correlation coefficient between the 20 year running means of +0.82), and reproduces the decline in decadal-mean West Amazonian rainfall from the 1920s to 1960. This suggests that longer-term variations in the north-south gradient across the Atlantic, and associated effects on Amazonian rainfall, are a consequence of forced as much as internal variability. Furthermore, the two model runs taken together indicate that non-greenhouse gas forcing, primarily from anthropogenic and volcanic aerosols, has acted to suppress the development of a stronger north-south gradient across the tropical Atlantic and thereby delayed the suppression of dry season rainfall in Western Amazonia. It seems that reflective sulphate aerosol pollution produced in the northern hemisphere may have helped to maintain rainfall in South America, just as it may have contributed to the Sahelian droughts of the 1970s and 1980s²².

The HadCM3LC model also produces a realistic correlation between interannual variations in the West Amazonian rainfall and the ANSG Index (Figure 3). The best-fit straight-lines linking these variables for the model and the observations are very nearly parallel (gradients of -0.65 ± 0.29 and -0.58 ± 0.46 mm day⁻¹ K⁻¹ respectively; here and elsewhere in this paper we quote error bars as ± 2 standard deviations giving approximately 95% confidence limits). HadCM3LC validates best amongst current GCMs in this respect (see Supplementary Information). In the 21st century the model simulates a strengthening of the relationship between decreasing West Amazonian rainfall for the July-October period and an increasing ANSG index, as indicated by the quadratic best-fit shown in Figure 3.

Our model simulations suggest that the north Atlantic region will warm more rapidly than the south Atlantic in the future, leading to a northward movement of the Intertropical Convergence Zone and suppression of July-October rainfall in West Amazonia. Aerosol pollution has occurred predominantly in the industrialised north, tending to suppress the development of this north-south warming gradient. However, as air quality improves, aerosol cooling of the climate is expected to decline⁹, potentially revealing a larger north-south gradient across the tropical Atlantic. This is evident in the HadCM3LC including aerosols (green line in Figure 2), which predicts a 2K increase in the ANSG Index by the end of this century. As a consequence, this GCM projection suggests that the conditions of 2005 will be experienced more and more frequently under increasing atmospheric greenhouse gas concentrations and reducing sulphur dioxide emissions in the northern hemisphere (see Supplementary Information).

Climate model projections are known to differ markedly with regard to regional rainfall changes over Amazonia but an intercomparison of the results from twenty GCMs included in the IPCC 4th Assessment Report reveals some robust features; (a) there is an across-model relationship between the 21st century trends in West Amazonian rainfall and the 21st century trends in the ANSG index - which is consistent with the observed interannual variability in these variables; and (b) models which include aerosol forcing tend to have greater increases in the ANSG index

in the first few decades of the 21st century (see Supplementary Information, Figure S3). Taken together, these findings support our basic conclusion that aerosol forcing has delayed reductions in Amazonian rainfall, but is unlikely to do so for much longer.

We estimated the probability of a “2005-like” year occurring in the HadCM3LC run with aerosols, based on the fraction of years in a centred 20-year window that exceed the ANSG Index for 2005 (Figure 4). The model suggests that 2005 was an approximately 1 in 20 year event, but will become a 1 in 2 year occurrence by 2025, and a 9 in 10 year occurrence by 2060. These thresholds obviously depend on the rate of increase of CO₂, which is itself dependent on the emissions scenario chosen. Figure 4(b) shows how the probability of a 2005-like event increases as a function of CO₂ concentration in HadCM3LC, with the 50% probability crossed at about 450ppmv, and the 90% probability crossed at around 610ppmv. These results suggest a rapidly increasing risk of 2005-like droughts in Amazonia under conditions of reducing aerosol loading and increasing greenhouse gases.

Methods Summary

The climate model used was HadCM3LC - a version of HadCM3¹⁹ which includes an interactive carbon cycle³. Two model runs were carried-out; one with greenhouse gases only³, and one with greenhouse gases plus other key climate forcing factors including anthropogenic sulphate aerosols⁸. In both model runs, atmospheric CO₂ concentration was modelled interactively by specifying emissions from the IS92a scenario and allowing the carbon cycle model to partition these between ocean, terrestrial and atmospheric carbon pools. Non-CO₂ GHGs were prescribed to follow a standard IS92a concentration scenario³. The “aerosol run” also included revised net CO₂ emissions from land-use, solar variability, tropospheric and stratospheric ozone changes, and the climatic effects of volcanic and anthropogenic aerosols⁸.

To investigate the relative importance of Atlantic and Pacific SST variability for Amazonian rainfall, we constructed SST indices from the Hadley Centre “HadISST” dataset¹⁷. The Pacific index was defined as the SST difference between the equatorial West Pacific (5°S-5°N, 120°E-180°E) and the Nino 3 region (5°S- 5°N, 150°W-90°W), to remove the impacts of global warming. The Atlantic index used was the “Atlantic North-South Gradient (ANSNG)” Index, defined as the SST difference between the tropical North Atlantic (15°N- 35°N, 75°W-30°W) and the tropical South Atlantic (25°S-5°S, 40°W-15°E). Time series of precipitation from the Climatic Research Unit²¹ (CRU TS 2.0) were calculated for Western Amazonia (75°W-60°W, 12°S-0°N). Linear regression analyses were carried-out to determine the relative-sensitivity of Western Amazonian rainfall to the Atlantic and Pacific SST indices. Rainfall in the dry season (July-October) was found to be correlated with variability in the ANSG Index, with no significant dependency on the E-W Pacific SST gradient¹⁶. This analysis therefore allowed us to focus on the Atlantic SST anomalies when seeking to understand the Amazonian drought of July-October 2005.

References

1. Melillo, J.M. *et al.*. Global climate change and terrestrial net primary production. *Nature* **363**, 234–240 (1993).
2. Tian, H. *et al.*. Climatic and biotic controls on annual carbon storage in Amazonian ecosystems. *Global Ecology and Biogeography* **9**, 315–335 (2000).
3. Cox, P.M., Betts, R.A., Jones, C.D., Spall, S.A. & Totterdell, I.J.. Acceleration of global warming due to carbon cycle feedbacks in a coupled climate model. *Nature*, **408**, 184-187 (2000).
4. Cox, P.M. *et al.*. Amazon dieback under climate-carbon cycle projections for the 21st century. *Theoretical and Applied Climatology*, **78**, 137-156 (2004).
5. Li, W., Fu, R., Dickinson, R.E.. Rainfall and its seasonality over the Amazon in the 21st century as assessed by the coupled models for the IPCC AR4. *Journal of Geophysical Research - Atmospheres*, **111**, Art. No. D02111 (2006).
6. Marengo, J.A., *et al.*. The drought of Amazonia in 2005. *Journal of Climate*, **21**, 495-516 (2008).
7. Marengo, J.A.. Interdecadal variability and trends of rainfall across the Amazon basin. *Theoretical and Applied Climatology*, **78**, 79-96 (2004).
8. Jones, C.D., Cox, P.M., Essery, R.L.H., Roberts, D.L., Woodage, M.. Strong carbon cycle feedbacks in a climate model with interactive CO₂ and sulphate aerosols. *Geophys. Res. Lett.* , **30** , 1479, doi:10.1029/2003GL016867 (2003).
9. Andreae, M.O., Jones, C.J., Cox, P.M.. Strong present-day aerosol cooling implies a hot future. *Nature*, **435**, 1187-1190 (2005).
10. Fu, R., Dickinson, R.E., Chen, M.X., Wang, H.. How do tropical sea surface temperatures influence the seasonal distribution of precipitation in the equatorial Amazon? *J. Climate*, **14**, 4003-4026 (2001).
11. Liebmann, B., Marengo, J.. Interannual variability of the rainy season and rainfall in the Brazilian Amazon basin. *Journal of Climate* **14**, 4308-4318 (2001).

12. Nobre, P., Shukla, J.. Variations of sea surface temperature, wind stress and rainfall over the tropical Atlantic and South America. *Journal of Climate* **9**, 2464-2479 (1996).
13. Meehl, G.A., Washington, W.M.. El Nino-like climate change in a model with increased atmospheric CO₂ concentrations. *Nature*, **382**, 56-60 (1996).
14. Folland, C.K., Colman, A.W., Rowell, D.P., Davey, M.K.. Predictability of Northeast Brazil rainfall and real-time forecast skill 1987-1998. *Journal of Climate*, **14**, 1937-1958 (2001).
15. Marengo, J.A., Liebmann, B., Kousky, V.E., Filizola, N.P., Wainer, I.C.. Onset and end of the rainy season in the Brazilian Amazon Basin. *Journal of Climate*, **14**, 833-852 (2001).
16. Harris, P.P, Huntingford, C., Cox, P.M.. Influence of Atlantic and Pacific SST on Amazon basin future climate change. *Phil. Trans. Roy. Soc.*, 10.1098/rstb.2007.0037 (2008).
17. Rayner N.A. *et al.* . Global analyses of sea surface temperature, sea ice, and night marine air temperature since the late nineteenth century. *Journal of Geophysical Research - Atmospheres*, **108**, Art No. 4407 (2003).
18. Good, P., Lowe, J., Collins, M., Moufouma-Okia, W., *in press*. An objective tropical Atlantic sea surface temperature gradient index for studies of South Amazon dry-season climate variability and change. *Phil. Trans. Roy. Soc.*, 10.1098/rstb.2007.0024 (2008).
19. Gordon, C. *et al.* Simulation of SST, sea ice extents and ocean heat transports in a version of the Hadley Centre coupled model without flux adjustments *Climate Dynamics*, **16**, 147-168 (2000).
20. Nakicenovic, N. *et al.*, *Special Report on Emissions Scenarios, Summary for Policy Makers*, Intergovernmental Panel on Climate Change, Geneva, Switzerland (2000).
21. New, M., Hulme, M., Jones, P.. Representing twentieth-century space-time climate variability. Part II: Development of 1901-96 monthly grids of terrestrial surface climate. *Journal of Climate*, **13**, 2217-2238 (2000).
22. Rotstayn, L.D., Lohmann, U.. Tropical rainfall trends and the indirect aerosol effect. *J. Climate*, **15**, 2103-2116 (2002).

Acknowledgements. The authors acknowledge funding from the NERC CLASSIC programme and Great Western Research (P.M.C. and T.E.J.); the CEH Science Budget (C.H. and P.P.H.); the UK Department for Environment, Food and Rural Affairs and UK Ministry of Defence (R.A.B, C.D.J. and M.C.); and the Brazilian Research Council and the Global Opportunity Fund from the UK Government (C.A.N. and J.A.M.). We also acknowledge the modeling groups, the Program for Climate Model Diagnosis and Intercomparison (PCMDI) and the WCRP's Working Group on Coupled Modelling (WGCM) for their roles in making available the WCRP CMIP3 multi-model dataset. Support of this dataset is provided by the Office of Science, U.S. Department of Energy.

Author Contributions. P.M.C. coordinated the work, identified the role of aerosols in delaying Amazonian drying in HadCM3LC, and drafted the paper; P.P.H. and C.H. defined the SST indices and analysed the relationships between these indices and West Amazonian rainfall, in both the observations and the model runs; C.D.J. and R.A.B. carried-out the HadCM3LC runs and provided output data from these runs; J.A.M. and C.A.N. provided observational data and insights on the nature of the 2005 drought in Western Amazonia; M.C. extracted and then inter-compared data on predicted changes in Amazonia from the CMIP3 models; C.H. and T.E.J. provided guidance on statistical significance.

Author Information. Reprints and permissions information is available at www.nature.com/reprints. The authors have no competing financial interests. Correspondance and requests for materials should be addressed to P.M.C. (p.m.cox@exeter.ac.uk)

Methods

Climate Simulations

The climate model used was HadCM3LC - a version of HadCM3¹⁹, but with a slightly lower ocean resolution (2.5° latitude by 3.75° longitude) which is required due to the extra computational expense of the ocean carbon cycle model. As a result the model requires the use of flux corrections. HadCM3LC includes interactive terrestrial and ocean carbon cycle components. The terrestrial carbon cycle model, TRIFFID, is a dynamic global vegetation model, which models carbon allocation between 5 competing plant functional types and a soil carbon reservoir²³. The ocean carbon cycle model, HadOCC, includes a representation of oceanic chemistry and biology²⁴.

In both model runs, atmospheric CO₂ concentration was modelled interactively and Non-CO₂ GHGs were prescribed to follow a standard IS92a concentration scenario³. The “aerosol run” in addition included⁸:

- The direct effect of anthropogenic sulphate aerosol was calculated using an interactive sulphur cycle scheme²⁵, driven by historic anthropogenic sulphur dioxide emissions and 21st Century anthropogenic emissions according to the SRES A2 scenario²⁰. Dry deposition was calculated separately for each of the 5 vegetation types in each gridbox, using CO₂-dependent canopy resistance values calculated by the MOSES-2 land-surface scheme²⁶.
- The first indirect effect of anthropogenic sulphate (i.e. the cloud albedo effect) was included using a non-interactive method in which cloud albedo perturbations are imposed based on output from a set of preliminary sulphur cycle runs²⁵.
- Climate forcing due to volcanic eruptions was represented by specifying the stratospheric aerosol distribution up to present day²⁷, and assuming it is zero thereafter.

- Tropospheric and stratospheric ozone changes were prescribed, based on results from the atmospheric chemistry model, STOCHEM²⁸.
- Solar forcing to present day was taken from a reconstruction of solar irradiances²⁹, and kept constant (equal to the mean of the last 11 years) after 2000.
- Revised net CO₂ emissions from land-use change⁸.

References

23. Cox, P.M.. Description of the TRIFFID dynamic global vegetation model. Hadley Centre Technical Note 24, Hadley Centre, Met Office (2001).
(http://www.metoffice.com/research/hadleycentre/pubs/HCTN/HCTN_24.pdf).
24. Palmer, J. R., Totterdell, I.J.. Production and export in a global ocean ecosystem model, *Deep Sea Res.*, **48**, 1169– 1198 (2001).
25. Johns, T. C. *et al.*. Anthropogenic climate change for 1860 to 2100 simulated with the HadCM3 model under updated emissions scenarios, *Clim. Dyn.*, **20**, 583-612 (2003).
26. Essery, R.L.H., Best, M.J., Betts, R.A., Cox, P.M., Taylor, C.M.. Explicit representation of sub-grid heterogeneity in a GCM land-surface scheme. *J. Hydrometeorol.* , **4** , 530-543 (2003) .
27. Sato, M., Hansen, J.E., McCormick, M.P., Pollack, J.B.. Stratospheric aerosol optical depths (1850 – 1990), *J. Geophys. Res.*, **98**, 22987 –22994 (1993).
28. Stevenson, D. S., Johnson, C.E., Collins, W.J., Derwent, R.G., Edwards, J.M.. Future estimates of tropospheric ozone radiative forcing and methane turnover: The impact of climate change, *Geophys. Res. Lett.*, **27**, 2073– 2076 (2000).
29. Lean, J., Beer, J., Bradley, R.. Reconstruction of solar irradiance since 1610: Implications for climate change, *Geophys. Res. Lett.*, **22**, 3195–3198 (1995).

Figure Captions

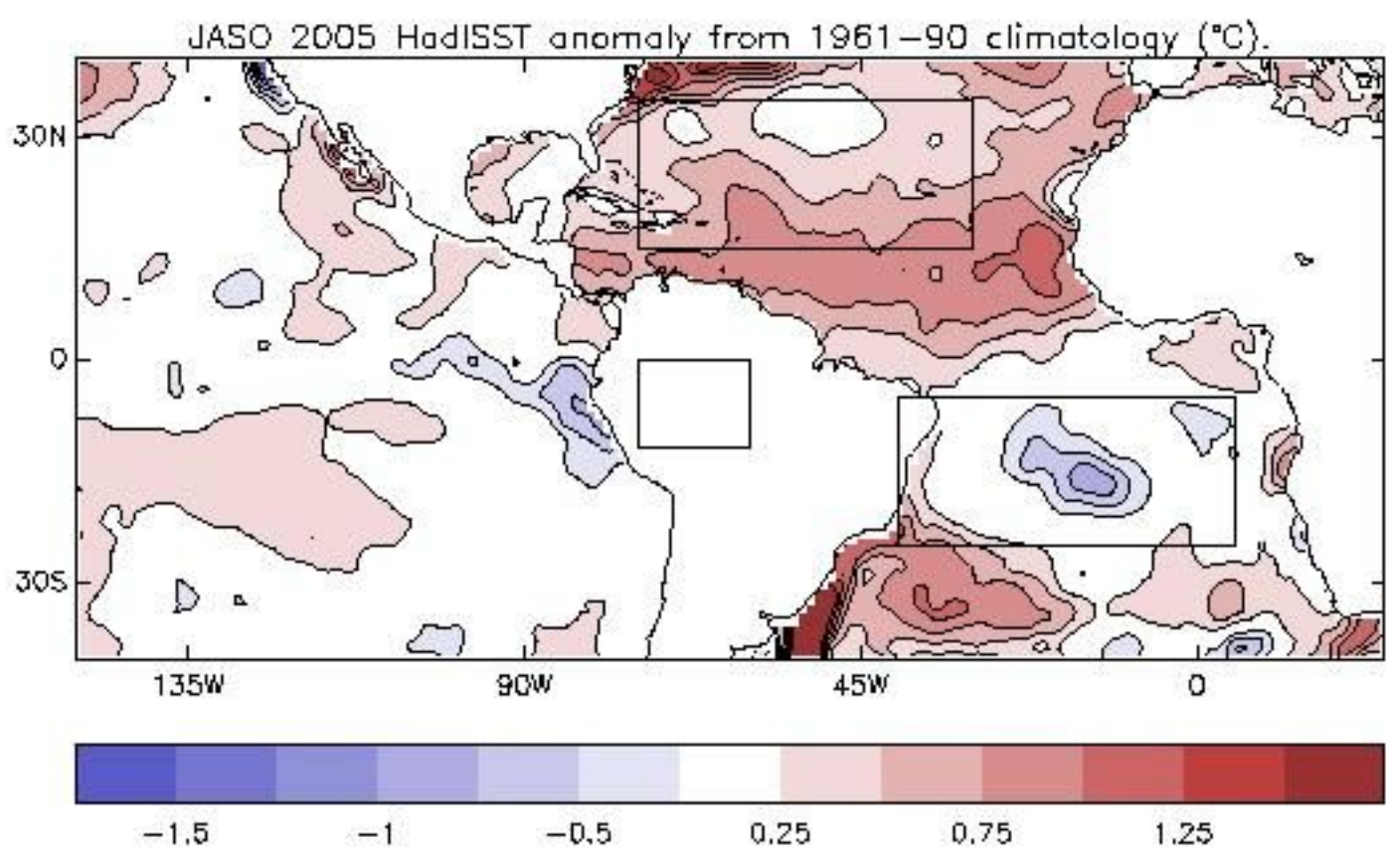
Figure 1: Anomalies in sea-surface temperatures for July-October 2005, relative to the July-October mean values over the standard climatological period of 1961-1990. The black boxes over the Atlantic show the definition of the “ANSG Index” : the north-south gradient across the Atlantic ocean ([15°N-35°N, 75°W-30°W] - [25°S-5°S, 40°W-5°E]). The box over the land shows the definition of Western Amazonia (75°W-60°W, 12°S-0°S) for the purpose of this study.

Figure 2: Comparison of observed and modelled climate variables relevant to the Amazonian drought of 2005. Evolution of July-October anomalies in (a) north-south SST gradient across the Atlantic ocean (“ANSG Index”); (b) rainfall in Western Amazonia. Observations are shown in black^{17,20}, with the thin line corresponding to annual values and the thick line showing 20-year running means. The other lines show decadal mean output from the HadCMLC GCM. The red line corresponds to a simulation of climate change driven by greenhouse gas increases only³, while the green line additionally includes changes in aerosols, stratospheric and tropospheric ozone, and revised fluxes of CO₂ from land-use change⁸. The large cross in (a) and the bar in (b) show the estimated values for July-October 2005.

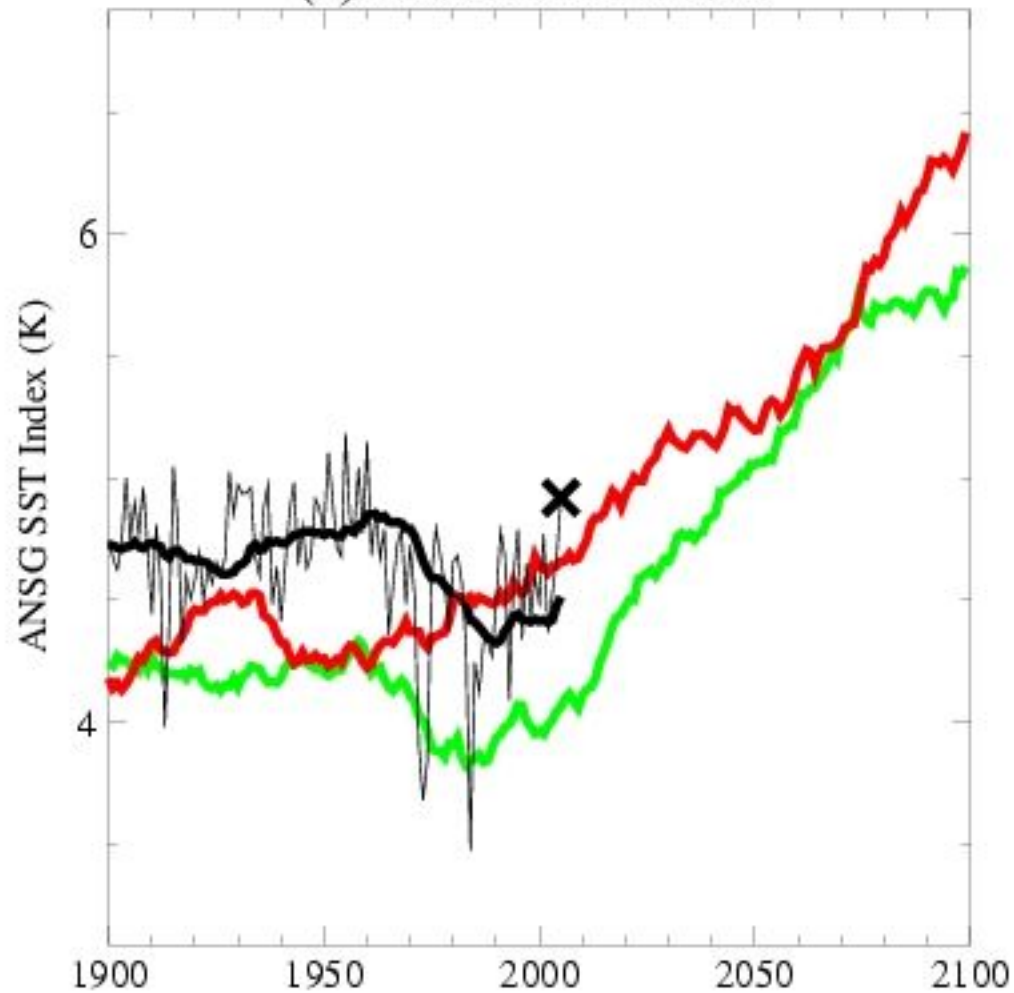
Figure 3: Relationship between July-October anomalies in rainfall in Western Amazonia and in the index of the north-south SST gradient across the Atlantic ocean (ANSG). Observations for the period 1901-2002 are shown by black diagonal crosses^{17,20}. Model output from the HadCMLC GCM simulation including aerosols⁸ is shown by black diamonds for the historical period (1901-2002) and by green diamonds for the simulation of the 21st century (2003-2100). The black continuous line shows the best fit straight line to the observations (1950-1999) and

the black dashed line shows the 20th century simulation (1900-1999). The green line shows the best quadratic fit to the entire GCM simulation (1860-2099). The large black cross shows the mean and standard deviation of the observations, and the red bar shows the range of estimated values for the 2005 Amazon drought.

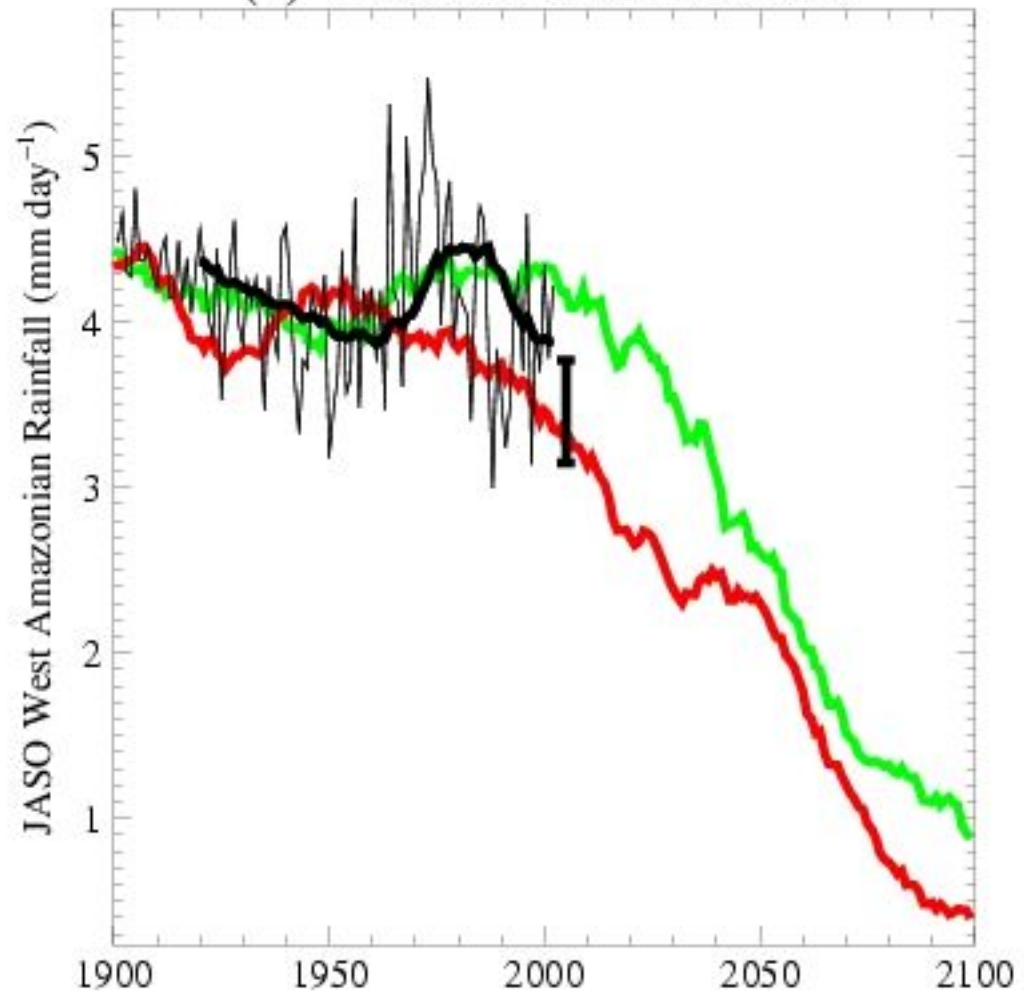
Figure 4: Predicted change in the probability of a 2005-like drought in Amazonia, based on results from the HadCM3LC GCM including aerosols⁸. Probabilities are calculated as the fraction of years that exceed the JASO 2005 anomaly in the ANSG Index, using the 20 years centred on each year: (a) Probability versus year; (b) Probability versus simulated CO₂ concentration. The dotted lines represent the point beyond which the 2005 anomaly is exceeded in 50% of the simulated years (year 2025, 450 ppmv of CO₂), and in 90% of the years (year 2060, 610ppmv of CO₂).



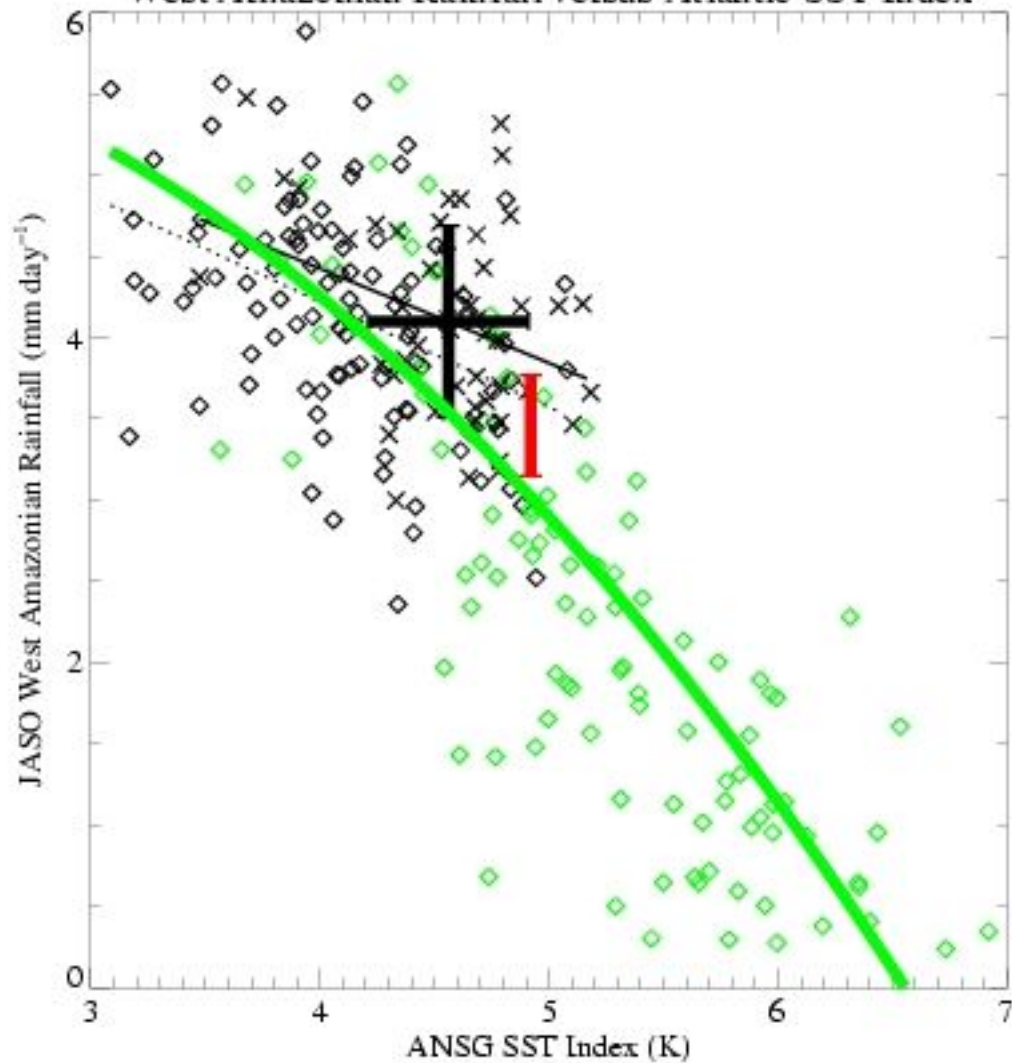
(a) Atlantic SST Index



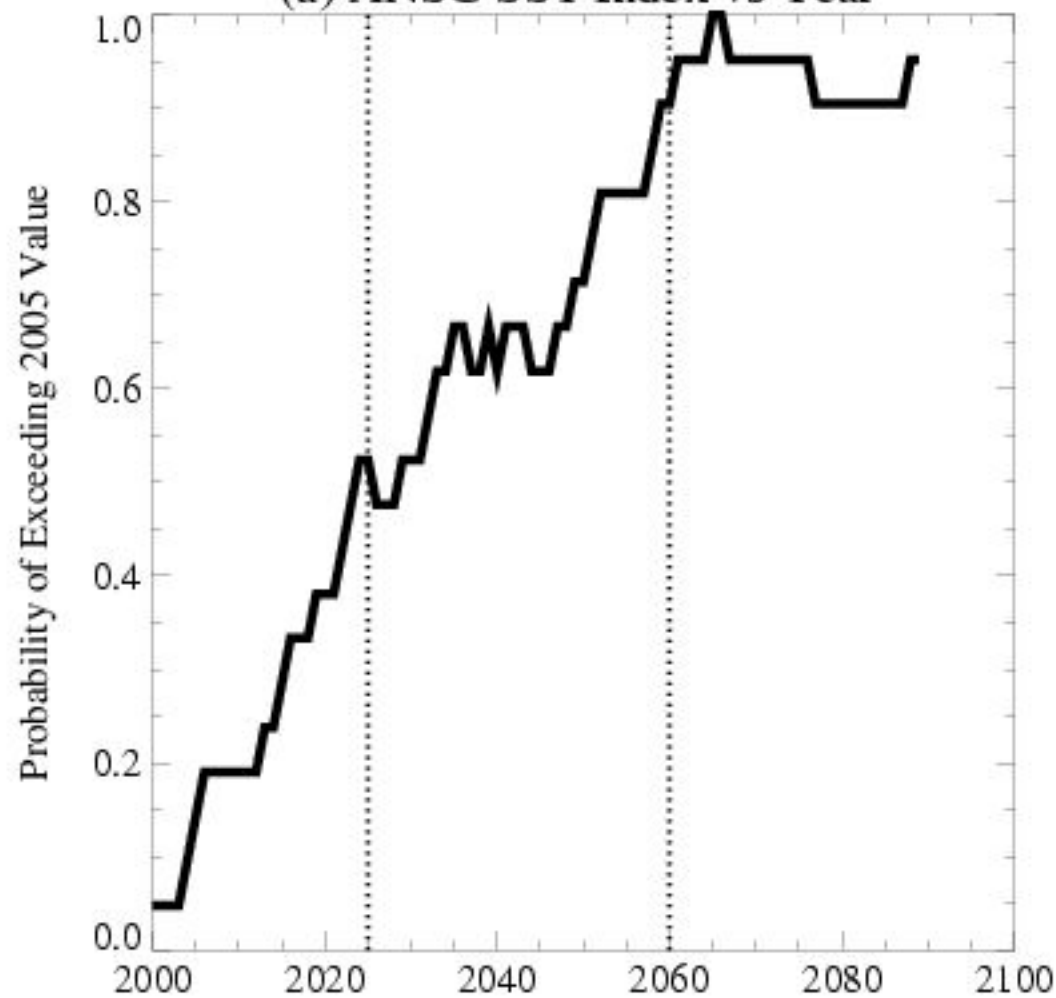
(b) West Amazonian Rainfall



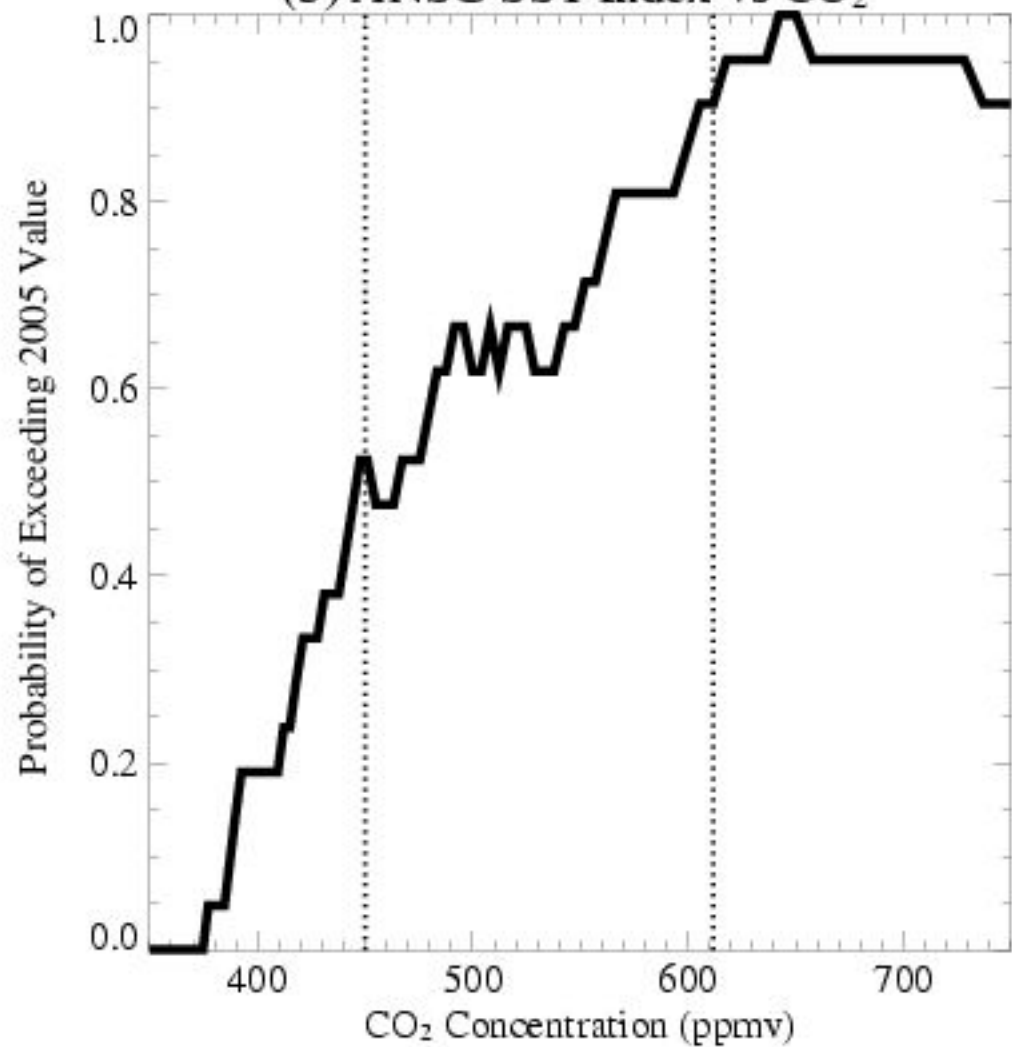
West Amazonian Rainfall versus Atlantic SST Index



(a) ANSG SST Index vs Year



(b) ANSG SST Index vs CO₂



Supplementary Information

1. Intercomparison of Amazonian Results from CMIP3 Global Climate Models

a) Simulated 20th Century Amazonian Climate

In order to put the results from HadCM3LC in context we compare results from twenty global climate models included in the CMIP3 archive (http://www-pcmdi.llnl.gov/ipcc/about_ipcc.php), that form the basis for the model projections included within the IPCC 4th Assessment Report. The models used here are listed in the caption to figure S1, and described at : http://www-pcmdi.llnl.gov/ipcc/model_documentation/ipcc_model_documentation.php

Figure S1 compares aspects of the mean 20th century Amazonian climate as simulated by the CMIP3 models against the observations^{1,2}, and against the 20th century simulation from the HadCM3LC model used in this study³. We use a meaning period of 1950-1999 for the observations to avoid difficulties with sparse Amazonian precipitation data in the first half of the 20th century.

The left panel of Figure S1 plots the modelled and observed mean values of the July-October West Amazonian precipitation against the mean values of the July-October ANSG Index (as defined in the caption to Figure 1). The dotted box shows the range of values that fall within two standard deviations of the observed values. Only two of the CMIP3 models, plus the Hadley Centre model used in this study (HadCM3LC – marked here with a green diamond), fall within these observational constraints.

The right panel of Figure S1 shows the linear regression between the interannual variability in the July-October West Amazonian rainfall and the interannual variability in the July-October ANSG, again versus the mean July-October ANSG. The y-values are equivalent to the gradient of the straight-lines shown in Figure 3 (where the continuous line in Figure 3 refers to the observations for 1950-1999, and the dashed-line refers to the HadCM3LC model for 1900-1999). The “P vs SST variability” values for the other CMIP3 models were derived in an identical way, *i.e.* by plotting the West Amazonian precipitation versus the ANSG index for each year and calculating the gradient of the best-fit straight-line. More of the CMIP3 models fit within the observational constraints in this case, in part because the observed mean value of this quantity has a relatively large standard deviation. The HadCM3LC model used in this study is unusual in being close to the best estimate of both the July-October West Amazonian rainfall, and the relationship between the interannual variability in this variable and the interannual variability in the July-October ANSG index.

b) Simulated 21st Century Amazonian Climate Change

Figure S2 shows the simulated trends in July-October West Amazonian rainfall and the July-October ANSG SST index, for each of the CMIP3 GCMs listed in the caption to Figure S1. The trends were calculated by fitting a quadratic to the annual values for 2000-2075 from simulations driven by the SRES A1B emissions scenario (which includes aerosols). The models differ markedly in their predictions of trends in these variables, with some models predicting increases in Amazonian rainfall and some reductions.

However, there is an across-model relationship between trends in the ANSG index and trends in West Amazonian rainfall – models in which the sub-tropical north Atlantic warms faster than the south tend to predict drying in Amazonia, and vice-versa. The best-fit straight-line linking these model trends of $0.53 \pm 0.42 \text{ mm day}^{-1} \text{ K}^{-1}$, is similar to the observed interannual relationship between these variables ($-0.58 \pm 0.46 \text{ mm day}^{-1} \text{ K}^{-1}$), suggesting a more robust relationship between the N-S gradient SST gradient in the Atlantic and the onset of the South American monsoon.

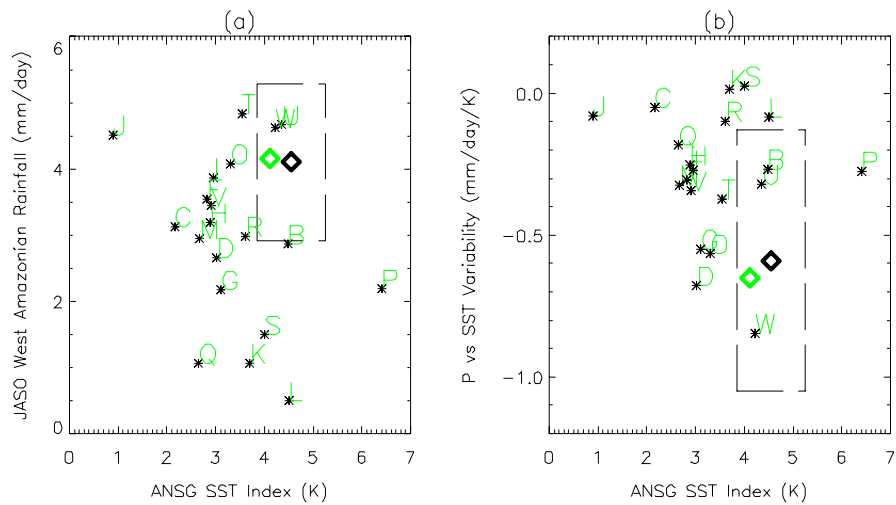


Figure S1 : Validation of GCM simulations of West Amazonian rainfall and the Atlantic N-S SST gradient (ANSG) index. The black diamond shows the best estimate from observations^{1,2}, and the dashed box represents plus and minus two standard deviations around this mean. The left panel shows July-October West Amazonian precipitation versus the ANSG Index. The right panel shows the relationship between the interannual variability in the rainfall and the interannual variability in the the ANSG versus, again versus the mean ANSG. The green diamond shows the results obtained with the GCM used in this study³. The 20th century simulations from CMIP3 GCMs are represented by the letters; B=BCCR-BCM2.0, C=CCSM3, D=CGCM3.1 (T47), F=CNRM-CM3, G=CSIRO-Mk3.0, H=ECHAM5/MPI-OM1, I=ECHO-G, J=FGOALS-g1.0, K=GFDL-CM2.0, L=GFDL-CM2.1, M=GISS-EH, O=INGV-SXG, P=INM-CM3.0, Q=IPSL-CM4, R=MIROC3.2 (hires), S=MIROC3.2 (medres), T=MRI-CGCM2.3.2, U=PCM, V=UKMO-HadCM3, W=UKMO-HadGEM1.

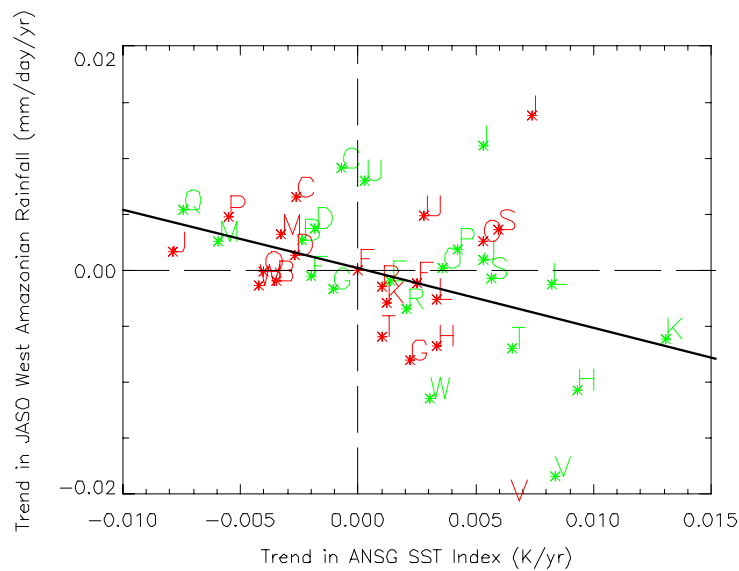


Figure S2 : Relationship between 21st century trends in West Amazonian rainfall and the Atlantic N-S SST gradient (ANSG) from the A1B simulations (green letters) and the 1% CO₂ per year simulations (red letters) of the twenty GCMs listed in the caption to Figure S1. The gradient of the overall best-fit straight-line is $-0.53 \pm 0.42 \text{ mm day}^{-1} \text{ K}^{-1}$, which is similar to the observed interannual relationship between these variables ($-0.58 \pm 0.46 \text{ mm day}^{-1} \text{ K}^{-1}$).

c) Effect of Aerosols on 21st Century Trends in the ANSG

It is apparent from Figure S2 that the CMIP3 models differ in the trends they project for West Amazonian rainfall and the ANSG SST index. However, the ensemble of model results support the hypothesis that increases in the ANSG index will reduce the July-October West Amazonian rainfall, in a manner similar to that experienced in 2005. Furthermore, these same models collectively produce a delay in warming of the north Atlantic relative to the south (as measured by the ANSG index) when aerosols are included in the climate simulations.

Figure S3 compares the trends in the July-October ANSG in simulations which either include (green lines) or exclude (red lines) the effects of aerosols. The lines are produced as means across the twenty CMIP3 models, smoothed using a 20-year running mean. The red lines come from simulations with an imposed 1% per year increase in atmospheric CO₂ concentration, and the green lines come from simulations consistent with the SRES A1B emissions scenario (including aerosol effects). Although these simulations are driven by different greenhouse gas concentrations they reach similar levels of total radiative forcing. We plot them on the same time axes to highlight the impact of anthropogenic aerosol pollution on the predicted evolution of the ANSG. The mean of the CO₂-only runs produces a negligible change in the ANSG in the future. In contrast the A1B runs show an upward trend in the first half of the 21st century from a minimum at around 1990. These results suggests that aerosols have acted to delay increases in the ANSG, but will cease to do so if anthropogenic sulphate emissions decline in the manner expected over the next 50 years.

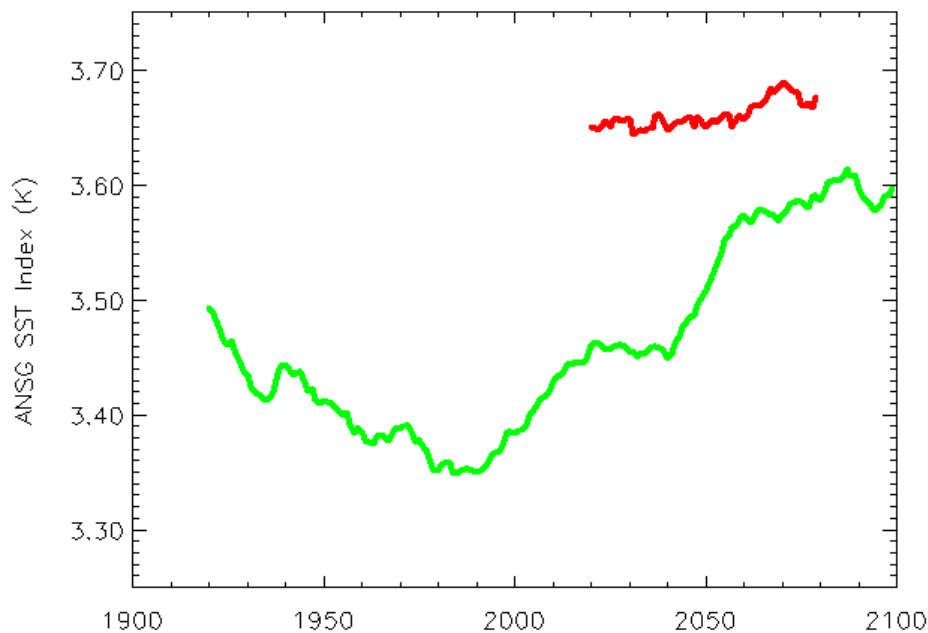


Figure S3 : Mean trends in the Atlantic N-S SST gradient (ANSG) index as simulated by models with (green line) and without (red line) sulphate aerosol forcing. These lines were calculated as 20-year running means across the twenty GCMs listed in the caption to Figure S1, using results from simulations driven by a prescribed 1% per year increase in CO₂ (red) and runs driven by the SRES A1B emissions scenario including aerosols (green).

2. Simulation of 20th Century Variation in the ANSG by HadCM3LC

Figure S4 compares the observed¹ and modelled³ (with HadCM3LC) evolution of the Atlantic N-S SST gradient (ANSG) through the 20th century. In both cases the y-axis is a 20-year running mean anomaly relative to the mean ANSG value over the period 1901-1951. The left hand panel is therefore essentially a magnification of Figure 2(a) showing just the period 1900-2000, and with the error in the model mean corrected. The right panel is a scatter plot of these modelled ANSG anomalies versus the ANSG anomalies as observed.

The model used in this study performs well in reproducing the long-term trends in the ANSG. The downward trend of the ANSG from 1900 to 1920 is well simulated, as is the subsequent upward trend until around 1960. The sharp drop in the ANSG from 1960 to 1980 and the increase from 1980 to the end of the century are slightly late in the model. However, it is remarkable that the overall shape of the observed variation in the ANSG can be reproduced so well in a relatively low-resolution climate model without detailed ocean-state initialisation. This suggests that decadal variability in the subtropical Atlantic is strongly forced by anthropogenic and volcanic aerosols.

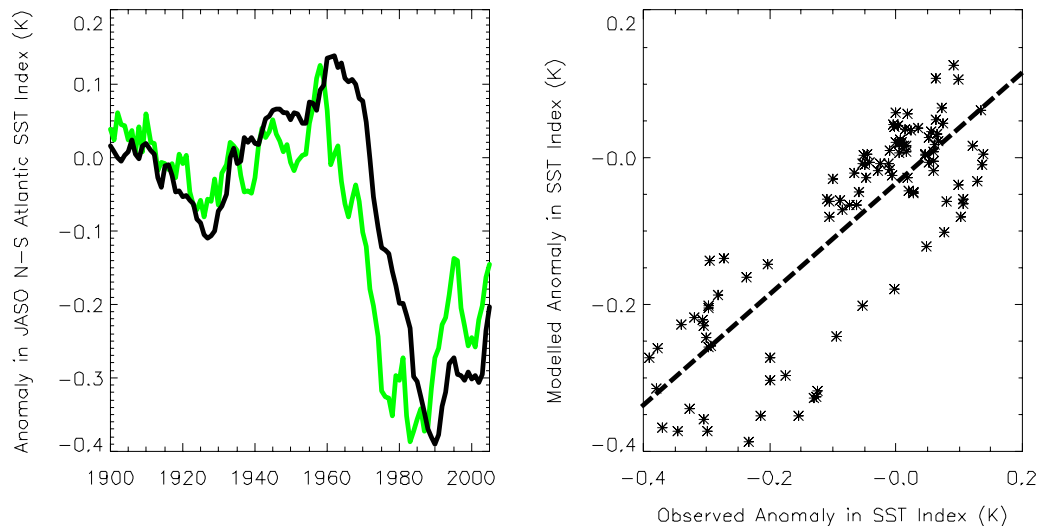


Figure S4: Observed and simulated variation in 20 year running-mean north-south SST gradient across the Atlantic ocean through the 20th century (as an anomaly relative to the respective means over the period 1901-1951). Observations are shown in black^{1,2} and the model used in this study is shown in green³ (left panel). The right panel shows the same data but as a scatter plot of the modelled versus predicted anomaly in the ANSG index.

References

1. Rayner N.A. *et al.* . Global analyses of sea surface temperature, sea ice, and night marine air temperature since the late nineteenth century. *Journal of Geophysical Research - Atmospheres*, **108**, Art No. 4407 (2003).
2. New, M., Hulme, M., Jones, P.. Representing twentieth-century space-time climate variability. Part II: Development of 1901-96 monthly grids of terrestrial surface climate. *Journal of Climate*, **13**, 2217-2238 (2000).
3. Jones, C.D., Cox, P.M., Essery, R.L.H., Roberts, D.L., Woodage, M.. Strong carbon cycle feedbacks in a climate model with interactive CO₂ and sulphate aerosols. *Geophys. Res. Lett.* , **30** , 1479, doi:10.1029/2003GL016867 (2003).